

# Finite element analysis for the equivalent stress on three-dimensional multiasperity coating

Xu Zhong\*, Wu Xiaoyan\*\*

\*School of Mechanical Engineering, Dalian University of Technology, Dalian, 116024, China,

E-mail: xuzhong@dlut.edu.cn

\*\*School of Mechanical Engineering, Dalian University of Technology, Dalian, 116024, China,

E-mail: wxy1111101@163.com

**crossref** <http://dx.doi.org/10.5755/j01.mech.18.3.1874>

## 1. Introduction

The stress distribution of multiasperity contact plays an important role in understanding most of the mechanisms in the case of friction, lubrication, and wear between the bodies in contact. Particularly, the stress analysis of the contact between rigid surface and coating surface is an essential part of the contact mechanics. There have been many models of elastic multiasperity contact established on the basis of the Hertz contact theory. For instance, different mathematical models were built respectively by Ioannides [1] and Lu Yan [2], which focused on the simulation of mechanical contact between two elastic rough surfaces. And they also discussed the effects of surface roughness on the surface deformation and stress.

With the further advance of the study on the contact problems, diverse kinds of rigid surfaces were involved in the contact with elastic surfaces. Komvopoulos [3, 4] and Reedy [5] analyzed the contact mechanism of the interface between the rigid surface with multiasperity and the elastic semiinfinite body. Yang Nan [6] investigated the elastic-plastic stress distribution on the rigid surface with a certain number of circular asperities, which contacts with the semiinfinite surface. And some researchers studied the contact between the rigid plane and other surfaces. Kogut [7] and Lin [8] made the 2D rigid plane contact with a single asperity and discussed this contact stress by thinning grid on the contact area. An elastic-plastic contact research had been carried out by Tong Ruiting [9], and the 2D contact between the rigid plane and the multiasperity coating was simulated. While Yeo et al [10] pointed out the relationship between the contact stress and the substrate deformation by analyzing a contact model of asperities, which described interfaces between the 2D rigid plane and great hardness asperities of the softer substrate. Those researchers almost studied the asperity contacts by the finite element method, as well as the virtual contact loading method [11] and the conjugate gradient method [12].

In a word, these current studies mainly look at the simplified stress model of the asperity contact between the rigid surface and the coating, and focus on the contact stress of the 2D rigid plane and the asperity. But the study on the contact stress of the 3D contact between the rigid plane and the multiasperity coating is hardly carried out. This unsolved problem has inhibited to realize the complicated nature of real contact situations at a certain extent.

In order to solve this problem, several models of the contact between the rigid plane and the multiasperity coating are established. And some parameters such as the

Young's modulus of coating, the spacing of asperities and the coating thickness are taken into consideration, their effects on the distribution of Von Mises stress (hereinafter referred as the equivalent stress) in the coating asperities and the coating/substrate interface are investigated in this work.

## 2. The finite element contact model

The 2D and 3D finite element models of the rigid plane in contact with the coating are established by using ANSYS 10.0, ANSYS Workbench 10.0 software. The contact model with only 9 asperities is researched to simplify the 3D multiasperity contact.

For the symmetric geometry of the model, it takes the 1/4 of this 3D model to form the computational field (shown in Fig. 1, a). The 2D contact model is composed of one side of this 3D contact model, which is AEFB plane in this article. And the asperity at the coating center is selected to form the single-asperity contact model. This work also refines the grid of the contact field shown in Fig. 1, b. Because the 2D model just involves the X-axis direction of the asperities in this 3D contact model, it can be viewed as a simplified form of this multiasperity contact for the comparative analysis. It is defined that the tangential direction is along the X-axis, the direction along the Y-axis is the normal. The distributions of the equivalent stress in the two tangential regions are analyzed respectively, which locate in the single asperity at the coating center (near the arc AP) and the coating/substrate interface (the segment DC).

In the Fig. 1, a,  $R$  is defined as the radius of the asperity,  $h$  is the asperity height, and  $l$  is the asperity spacing,  $d$  is the indentation depth of the rigid plane. Then the roughness of different coating surfaces can be simulated by the variety of  $l/R$ : the greater  $l/R$  stands for larger roughness and vice versa [6]. The negative displacement  $d/h$  along the z-axis is imposed on the coating by the rigid plane. The different values of  $d/h$  represent correspondingly indentation depths. In this model, those factors are definite, such as  $R = 100 \mu\text{m}$ ,  $h = 2 \mu\text{m}$ . As shown in Fig. 1, a, some structure sizes are decrease, like  $l_{EF} = l_{IE} = 100 \mu\text{m}$ , the coating thickness  $\delta_C = 20 \sim 40 \mu\text{m}$ , the substrate thickness  $\delta_S = 100 \mu\text{m}$ . And these asperities in the model are arranged in a square. For the asperity in vertex A fixed at the center of this model,  $l$  can be viewed as the center distance from the central asperity to the tangential and normal adjacent asperity. After refining the grid of asperities on the coating, the number of nodes is 10935 in the 2D model,

the 3D model has 20279 nodes, while it has 16958 nodes in the signal asperity model.

### 3. Results and analyses

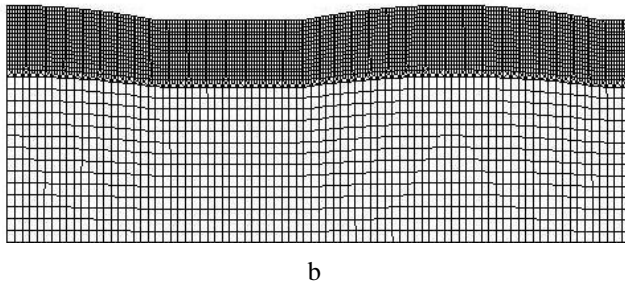
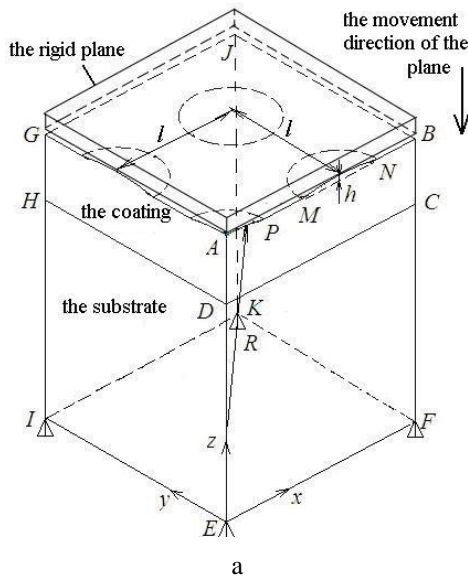


Fig. 1 The computational field of the multisasperity model: a - geometry of coating and substrate; b - the refined grid of asperities

The materials' properties of the coating and the substrate are shown in the bellow Table. It is defined obviously that  $E_C$  is the Young's modulus of the coating,  $E_S$  is Young's modulus of the substrate, and  $E_C/E_S$  is the Young's modulus ratio of those two parts. In this finite element analysis, the ceramic coating  $Si_3N_4$  and the ceramic coating WC can be defined as elastic material because of their high hardness. The substrate body consists of the bearing steel 52100. The ideal material of the substrate is assumed:  $E_T = 0$ , which is the elastic-plastic tangential modulus used to measure the degree of strain hardening [13].

Table

The materials' properties of the coating and the substrate

Materials	Yield strength $\sigma_Y$ , MPa	Tangent modulus $E_T$ , MPa	Poisson's ratio $\nu$	Young's modulus $E$ , MPa
The ceramic coating $Si_3N_4$	---	---	0.3	310000
The ceramic coating WC	---	---	0.3	450000
52100 steel	600	0	0.3	200000

Fig. 2, a gives the comparison of the distribution of tangential equivalent stress in the multisasperity ceramic coating  $Si_3N_4$  under different indentation depths and different models' dimensions ( $D = 2, D = 3$ ). And some parameters preliminarily determined are  $E_C/E_S = 1.55$ ,  $l/R = 0.6$ ,  $\delta_C = 30 \mu m$ . Here  $D = 2, d/h = 0.1$  represents the equivalent stress distribution of the 2D model ( $D = 2$ ) under the condition  $d/h = 0.1$ . In this figure, the Von Mises stress distribution of asperities on the 2D and 3D coating surfaces corresponds with the stress distribution concluded by Hertz. The shear stress of coating asperities increases with the increase of  $d/h$ , and the stress gradient changes greatly when it approaches to the center asperity. The maximum equivalent stress of the 3D contact model is greater than that of the 2D contact under the same condition, such as the Young's modulus of contact materials and the indentation depth of the rigid plane. There are two reasons mainly responsible for these results. Firstly, the stress of other asperities on the coating surface affects the center asperity's stress. In addition, the stress superposition of the tangential asperities appears when we investigate the equivalent stress in the 3D model.

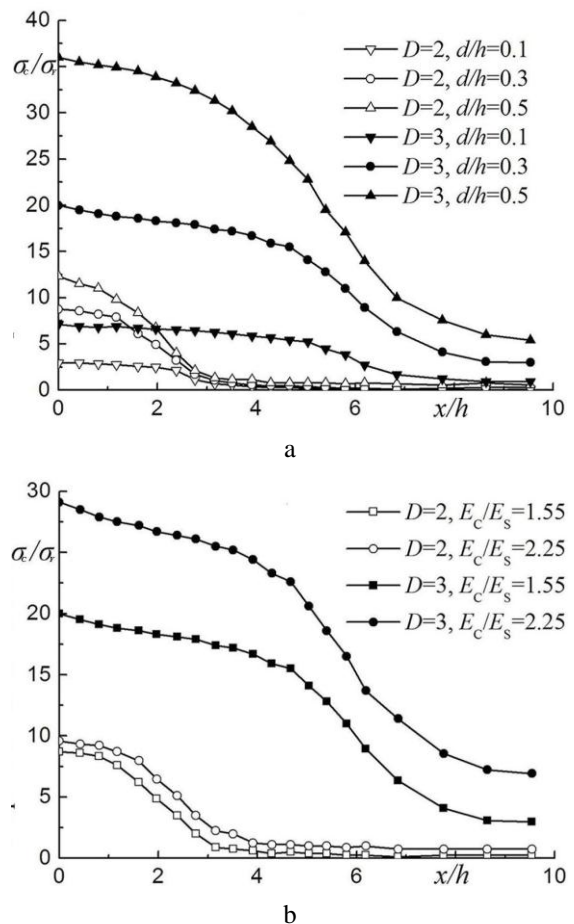


Fig. 2 The distribution of the equivalent stress in the asperity coatings ( $D = 2, 3$ ): a - under the different indentation depths; b - under the different Young's modulus ratio

As shown in Fig. 2, b, the comparison of two different multisasperity coatings on the equivalent stress distribution is presented. And some preconditions are deter-

mined as bellow:  $d/h = 0.3$ ,  $l/R = 0.6$ ,  $\delta_C = 30 \mu\text{m}$ . The equivalent stress of nodes in the 2D asperity coating all increases with the increase of  $E_C/E_S$ , and homogeneously this law can be applied to the 3D coating. Due to the 2D model, it is impossible to describe adequately real contact of multi-asperities and can not integral display the stress superposition of the asperities on coating surface, the equivalent stress in the 3D model at  $E_C/E_S = 1.55$  is much greater than that in the 2D model.

The distributions of the equivalent stress in the 3D single-asperity coating and the 3D multiasperity coating are shown in Fig. 3. When  $d/h = 0.3$ ,  $l/R = 0.6$ ,  $\delta_C = 30 \mu\text{m}$ , the equivalent stress on nodes of the single-asperity and the multiasperity surface increases with the increase of  $E_C/E_S$ , which can be viewed as the increased elastic modulus of the coating at the unchangeable substrate. But as the single-asperity has no near asperities to superimpose their stress, the equivalent stress of nodes in the single-asperity coating is greater than that in the multi-asperity with the invariable value of  $E_C/E_S$ .

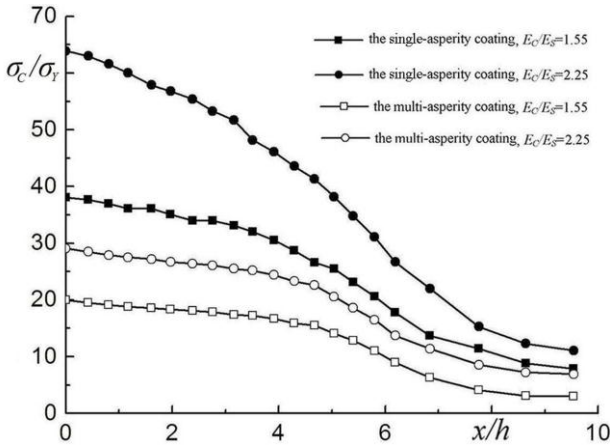


Fig. 3 The distribution of the equivalent stress in the coatings with the different number of the asperities

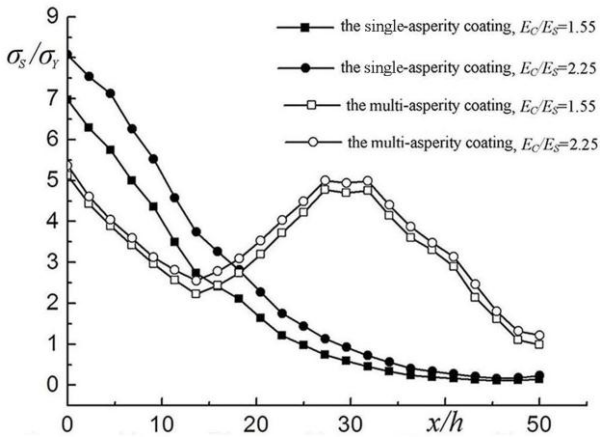


Fig. 4 The distribution of the equivalent stress on the coating/substrate interface

The distribution of equivalent stress on the coating/substrate interface is described in Fig. 4. For the single-asperity model, the maximum equivalent stress on the interface is at  $x/h = 0$  (under the center of this signal asperity), and the equivalent stress becomes smaller and smaller with the greater distance away from the center. But for the multiasperity, the maximum stress in each asperity follows

the same discipline compared with the asperity of the single-asperity model, and the minimum stress on the region between asperities is greater than that on the interface edge ( $x/h = 50$ ). With the increase of  $E_C/E_S$ , the equivalent stress on nodes of the single-asperity model all increases, and the growth rate is greater than that of the multiasperity, which conforms to the law shown in the Fig. 3. The main reason is that, at the same indentation depth, the contact area of the single-asperity model is less than that of the multiasperity obviously, but more surface stress of the signal asperity transfers to the coating/substrate interface. Considering the negative effect on the bonding strength of the interface (such as the interface crack caused by coating flaking) from the increase of the equivalent stress, the multiasperity coating with lower elastic modulus (such as the ceramic coating  $\text{Si}_3\text{N}_4$ ) can be praised in this paper.

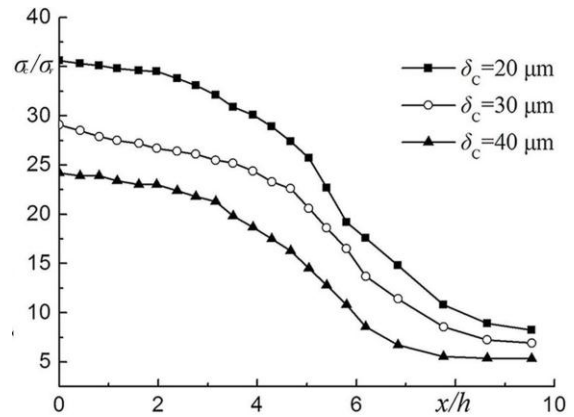


Fig. 5 The distribution of the equivalent stress in the multi-asperity coating (with different coating thicknesses)

Fig. 5 presents the distribution of the equivalent stress in the 3D multiasperity coatings with initial conditions:  $E_C/E_S = 2.25$ ;  $d/h = 0.3$ ;  $l/R = 0.6$ . Some values of the coating thickness  $\delta_C$  are fixed, such as  $20 \mu\text{m}$ ,  $30 \mu\text{m}$  and  $40 \mu\text{m}$ . The equivalent stress in the peak of the asperity is maximal, and it decreases with the longer distance from the center. The stresses on nodes of the coating surface all increase and the stress gradient becomes greater with the loss of  $\delta_C$ . That's mainly because the decreased  $\delta_C$  makes the equivalent stress increases, which acts on the external and internal coating in each unit area. And the stress distribution of the coating/substrate interface is showed in the Fig. 6.

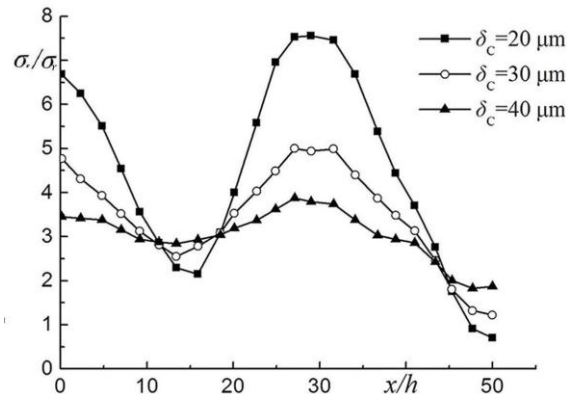


Fig. 6 The stress distribution of the coating/substrate interface (with different coating thicknesses)

With the decrease of  $\delta_C$ , the equivalent stress in the region under the asperity peak increases and the stress gradient increases as well. Because of the stress superposition of surrounding asperities in the contact area, the stress on the region between the asperities is greater than that on the interface edge. And the bonding strength of the coating/substrate interface can be enhanced by increasing the coating thickness to avoid the harmful influences of the equivalent stress on the bonding properties of this interface.

Fig. 7 is the relation curve of the maximum equivalent stress and the spacing between coating asperities for the coating surface. The preconditions of this curve are listed below:  $E_C/E_S = 2.25$ ,  $d/h = 0.3$  and  $\delta_C = 30 \mu\text{m}$ . And the y-axis represents the ratio of two maximum equivalent stress values  $\sigma_{cm,max}$ ,  $\sigma_{cs,max}$ , which grow out of the multiasperity coating surface and the single-asperity coating surface. It can be seen that the maximum equivalent stress of the coating increases with the increase of  $l/R$  due to the reduced interaction of coating asperities correspondingly.

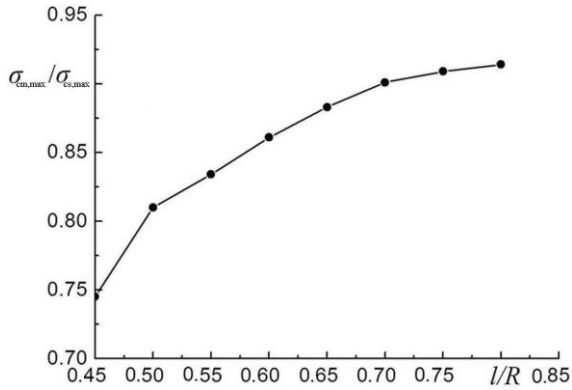


Fig. 7 The relation curve of the maximum equivalent stress and the spacing between coating asperities (on the coating surface)

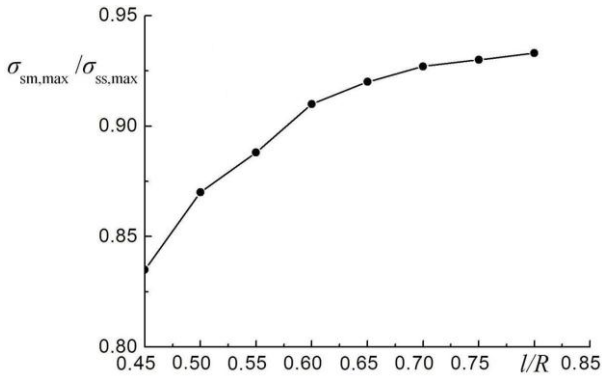


Fig. 8 The relation curve of the maximum equivalent stress and the spacing between coating asperities (in the coating/substrate interface)

Fig. 8 is the relation curve of the maximum equivalent stress and the spacing between coating asperities for the coating surface. The y-axis is defined as the ratio of two maximum equivalent stress values  $\sigma_{cm,max}$ ,  $\sigma_{cs,max}$ , and they respectively come from the interfaces of the multiasperity model and the single-asperity model. From this figure, with the increase of  $l/R$ , the maximum equivalent stress of the interface slightly increases owing to the reduction of the stress superposition, which is simi-

lar to this stress change shown in Fig. 7 at the same preconditions.

From Figs. 2, 3, 5 and 7, a multiple linear regression equation can be concluded to depict the maximum equivalent stress on the asperity coating surface. The equation is given as below

$$\sigma_c = 434.41 \left( \frac{E_C}{E_S} \right)^{0.486} \delta_C^{-0.553} \left( \frac{l}{R} \right)^{0.317} \left( \frac{d}{h} \right)^{0.999} \quad (1)$$

Here  $E_C/E_S$  is the Young's modulus ratio of the coating/substrate interface,  $\delta_C$  is the coating thickness, and  $l/R$  is defined as the spacing ratio of asperities,  $d/h$  is the ratio of the indentation depth of the rigid plane to the height of the asperity.

Eq. (1) can be verified highly significant by the  $F$  method. In order to eliminate the effects of the random error, variance analysis is used in this article. And the results show that the effects on the maximum equivalent stress of the asperity surface amount decrease in order of  $d/h$ ,  $\delta_C$  and  $l/R$ .

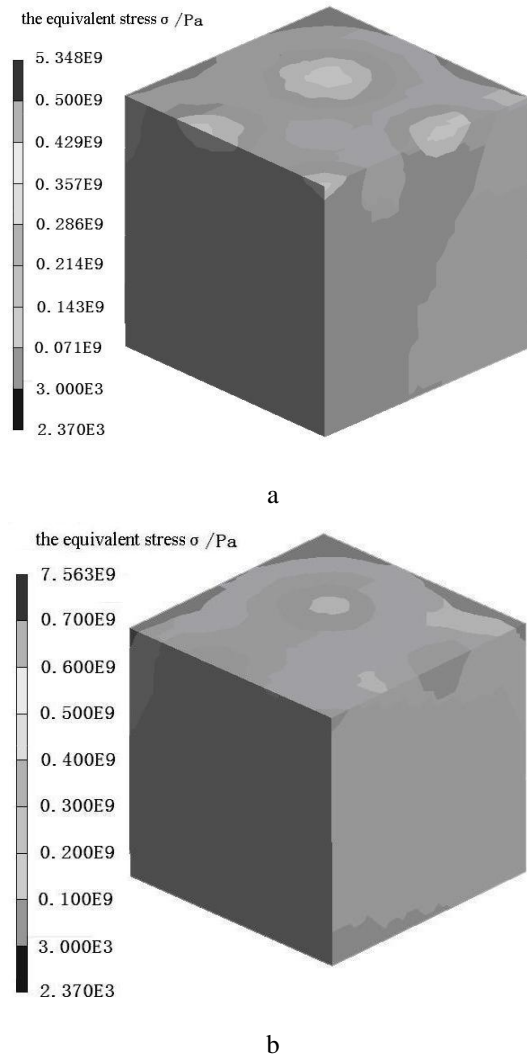


Fig. 9 The equivalent stresses of the coating/substrate interfaces: a -  $E_C/E_S = 1.55$ ; b -  $E_C/E_S = 2.25$

The equivalent stresses of the coating/substrate interfaces are shown respectively in Figs. 9, a and b at  $E_C/E_S = 1.55$ , 2.25 under these fixed factors, such as



$l/R = 0.6$ ,  $d/h = 0.2$ ,  $\delta_C = 30 \mu\text{m}$ . It is found that the gradient of this equivalent stress decreases with the increase of  $E_C/E_S$ , but the stress on substrate surface of some local region corresponding to the asperities increases a little when it is below the yield strength. Because of the greater elastic modulus of the coating, its resistance to deformation has enhanced, and the coating deformation decreases at the same indentation depth, then the stress on the substrate surface can distribute evenly.

#### 4. Conclusions

1. The equivalent stress of three-dimensional asperity coating is greater than that of the 2D model under the changes of the indentation depth and the Young's modulus, due to the response to the resultant force of all asperities on the coating surface.

2. Increasing the coating thickness, while reducing the indentation depth of rigid plane, the asperity spacing, and the Young's modulus ratio of the coating/substrate interface can make the maximum equivalent stress significantly reduced.

3. The bonding strength of the coating/substrate interface can be improved by increasing the number of coating asperities and the coating thickness and reducing the Young's modulus of the coating. Under the same indentation depth, the increase of the coating's Young's modulus makes the coating deformation decline. And the deformation of the coating which is between two adjacent asperities located on different tangent plane decreases with the increasing spacing of these two asperities.

#### Acknowledgements

This research is supported by the National Natural Science Foundation of China under the contract number 51075052, and the science and technology planning project of Dalian City under the contract number 3001052003.

#### References

1. **Ioannides, E.; Kuijpers, J.C.** 1986. Elastic stresses below asperities in lubricated contacts, *ASME Journal of Tribology* 108: 394-402. <http://dx.doi.org/10.1115/1.3261213>.
2. **Lu Yan; Liu Zuomin** 2010. Friction surface contact deformation model based on material thermal parameters, *Journal of Mechanical Engineering* 46(9): 120-125. <http://dx.doi.org/10.3901/JME.2010.09.120>.
3. **Komvopoulos, K.** 1988. Finite element analysis of a layered elastic solid in normal contact with a rigid surface, *ASME Journal of Tribology* 110: 477-485. <http://dx.doi.org/10.1115/1.3261653>.
4. **Komvopoulos, K.; Choi, D.H.** 1992. Elastic finite element analysis of multiasperity contacts, *ASME Journal of Tribology* 114: 823-831. <http://dx.doi.org/10.1115/1.2920955>.
5. **Reedy, E.D.** 2006. Thin-coating contact mechanics with adhesion, *Journal of Materials Research* 21(10): 2660-2668. <http://dx.doi.org/10.1557/jmr.2006.0327>.
6. **Yang Nan; Chen Darong; Kong Xianmei** 2000. Elastic-plastic finite element analysis of multiasperity contacts, *Tribology* 20(3): 202-206.

7. **Kogut, L.; Etsion, I.** 2002. Elastic-plastic contact analysis of a sphere and a rigid flat, *Journal of Applied Mechanics* 69: 657-662. <http://dx.doi.org/10.1115/1.1490373>.
8. **Lin, L.P.; Lin, J.F.** 2006. A new method for elastic-plastic contact analysis of a deformable sphere and a rigid flat, *ASME Journal of Tribology* 128: 221-229. <http://dx.doi.org/10.1115/1.2164469>.
9. **Tong Ruiting; Liu Geng; Liu Tianxiang** 2007. Mechanic analysis of two-dimensional elasto-plastic contact with multiasperity coating surfaces, *Mechanical Science and Technology* 26(1): 21-24.
10. **Yeo, C.D.; Katta, R.R.; Lee, J.** 2010. Effect of asperity interactions on rough surface elastic contact behavior: Hard film on soft substrate, *Tribology International* 43: 1438-1448. <http://dx.doi.org/10.1016/j.triboint.2010.01.021>.
11. **Zhao Hua; Yang Yiren; Jin Xueyan** 2000. Analysis of elastic-plastic contact stress in thick oxidized sheet, *Tribology* 20(2): 135-138.
12. **Meng Fanning; Hu Yuanzhong; Wang Hui** 2008. Effect of filter cut off frequency on contact mechanism between rough surfaces, *Journal of Mechanical Engineering* 44(10): 104-107.
13. **Liu Geng; Zhu Jun; Yu Lie** 2001. Elasto-plastic contact of rough surfaces, *STLE Journal of Tribology Transactions* 44(3): 437-443. <http://dx.doi.org/10.1080/10402000108982478>.

Xu Zhong, Wu Xiaoyan

TRIJŲ DIMENSIJŲ KINTAMO NELYGUMO DANGOS EKVIVALENTINIŲ ĮTEMPIŲ TYRIMAS BAIGTINIŲ ELEMENTŲ METODU

R e z i u m ė

Tampriems kintamo nelygumo kontaktams tarp dvimačių ir trimačių modelių standžios plokštumos ir dangos paviršiaus nustatyti taikomas baigtinių elementų metodas. Nustatyta, kad tamprumo modulių santykio pasikeitimas, dangos storis, nelygumų išsidėstymas, standžios plokštumos įsiskverbimo gylis turi įtakos bendram deformacijos ir įtempių pasiskirstymui dangos nelygumuose ir dangos bei pagrindo skiriamajame paviršiuje. Rezultatai rodo, kad ekvivalentiniai įtempiai 3D kontakto modelyje yra didesni nei 2D modelyje ir priklauso nuo įtempių pasiskirstymo nelygumuose. Išmatuota maksimalių ekvivalentinių įtempių 3D kontakto modelyje priklausomybė nuo kintamo įsiskverbimo gylio efekto, dangos storio, tamprumo modulių santykio, nelygumų išdėstymo. Kuo mažesnis tamprumo modulių santykis, įsiskverbimo gylis, nelygumų erdviškumas ir kuo didesnis dangos storis, tuo mažesni ekvivalentiniai įtempiai dangos paviršiuje. Dangos ir pagrindo ryšio jėgos aiškiai sumažėja didėjant nelygumų skaičiui ir dangos storiui, mažėjant tamprumo modulių santykiui.

Xu Zhong, Wu Xiaoyan

FINITE ELEMENT ANALYSIS FOR THE  
EQUIVALENT STRESS ON THREE-DIMENSIONAL  
MULTIASPERITY COATING

S u m m a r y

The finite element method is applied to establish two-dimensional and three-dimensional models of elastic multiasperity contact between the rigid plane and the coating surface. It is found that the changes of Young's modulus ratio, coating thickness, spacing of asperities and indentation depth of the rigid plane influence the total deformation and stress distribution in coating asperity and coating/substrate interface. The results show that the equivalent stress of 3D contact model is greater than that

of 2D model due to the stress superposition of asperities. For 3D contact model, the effects of varied levels of indentation depth, coating thickness, Young's modulus ratio, spacing of asperities on the maximum equivalent stress are measured. And the smaller the Young's modulus ratio, indentation depth, spacing of asperities and the larger the coating thickness, the smaller the maximum equivalent stress in the coating surface. The coating/substrate bonding strength has been up-graded obviously by increasing the number of asperities and the coating thickness, reducing the Young's modulus ratio.

**Keywords:** Multiasperity coating, three-dimensional contact model, equivalent stress, finite element method.

Received March 18, 2011

Accepted May 30, 2012